Photochemistry of Metal-Metal Bonded Compounds. I. Isolation and X-Ray Molecular Structure Analyses of Orthometalated Triphenyl Phosphite Manganese Carbonyl Derivatives and Reaction Mechanisms of Orthometalation from Photodegradation of Manganese Carbonyl Derivatives with Sn–Mn Bond

Satoru ONAKA,* Yoshinori KONDO, Nobuhiro FURUICHI,
Koshiro TORIUMI,† and Tasuku ITO†

Department of Chemistry, Nagoya Institute of Technology, Gokisocho, Showa-ku, Nagoya 466
† *Division of Applied Molecular Science, Institute for Molecular Science, Myodaiji, Okazaki, 444*

(Received March 5, 1982)

Photochemical degradation of a series of tin-manganese bonded complexes was studied. The apparent reactivity of the tin-manganese bond toward UV irradiation is interpreted on the basis of absorption spectra of relevant complexes and available emissions from the light source. Two kinds of orthometalated products were obtained from photolysis of Me_3Sn–$Mn(CO)_3[P(OPh)_3]_2$ in benzene. Various kinds of experiments suggest that their photochemical reactions proceed through homolytic cleavage of the Sn–Mn bond in the initial stage and the resulting 15-electron intermediates abstract hydrogen from the triphenyl phosphite moiety. Molecular structures of the two kinds of orthometalated products, as clarified by X-ray structure analyses, are described.

There is much current research activity on photochemical reactions of metal-metal bonded complexes.[1,2] The impetus behind these studies is to understand the photochemistry of these complexes in connection with excited states and/or to obtain new intriguing derivatives by exploiting photochemically generated unstable intermediates.[1,2] Although the ultimate goal of these studies is to predict theoretically, and to design or control, photochemical reactions for these complexes, only limited understanding of photochemical reaction mechanisms with regard to the photochemical excitation has been obtained up to the present.[1,2] Those metal carbonyl derivatives which possess transition metal-transition metal bonds and transition metal-group IV metal bonds, have so far been explored intensively.[1-3] We have been studying structures, bondings, and syntheses of manganese carbonyl derivatives which have manganese-group IV metal atom bonds.[4] As part of a systematic investigation on structure, bonding, and reactivity of the aforementioned type of manganese carbonyl derivatives, we were led to investigate photochemical behavior of this series of compounds.

According to Wrighton *et al.*,[5] the photochemistry of group IV metal-transition metal bonds for Ph_3M'–$M(CO)_3L$ (M′=Ge and Sn; M=Mn and Re) is dependent on L, M′, and M, and the initial photochemical process is the charge transfer from the M′–M bond (HOMO) to the π^* of L (LUMO) which leads to labilization of the M′–M bond. Reichel and Wrighton,[6] however, have demonstrated that the main result of photoexcitation of R_3Si–$Co(CO)_4$ (R=Ph and Et) is dissociative loss of CO. These studies suggest that the photochemical behavior of the transition metal-group IV metal bond in R_3M'–$M(CO)_xL_y$ type compounds is very much dependent on the substituent of L on the transition metal atom M, the group IV metal atom M′, and the transition metal atom M itself, and that the photochemical behavior can be interpreted in terms of the molecular orbital diagram. When L has no low-lying empty π^* orbital, the lowest energy excitation for M=Mn or Re is the $d\pi \rightarrow \sigma^*$ or $\sigma_b \rightarrow \sigma^*$(M′–M) transition, which may depends on the sp^3 level of atom M′ (Schemes 1(a) and (b)).[5,6] Scheme 1(a) may hold for M′=Si and Scheme 1(b) for M′=Sn. In the combination of M′=Sn and L which has a low-lying empty π^* orbital, the lowest energy excitation is the $\sigma_b \rightarrow \pi^*$(L) transition (Scheme 1(c)).[5,6] It comes out from Scheme 1 that photochemical cleavage of the M′–M bond becomes efficient, which is otherwise reluctant, when the M′–M bond strength is affected by replacing R or L with another substituent and the $\sigma_b \rightarrow \sigma^*$ (M′–M) transition approaches to available excitation energy. In this regard, the manganese-tin bonds in R_3Sn–$Mn(CO)_xL_y$ and $R_{4-x}Sn[Mn(CO)_5]_x$ are enticing candidates to examine this idea; our previous spectro-

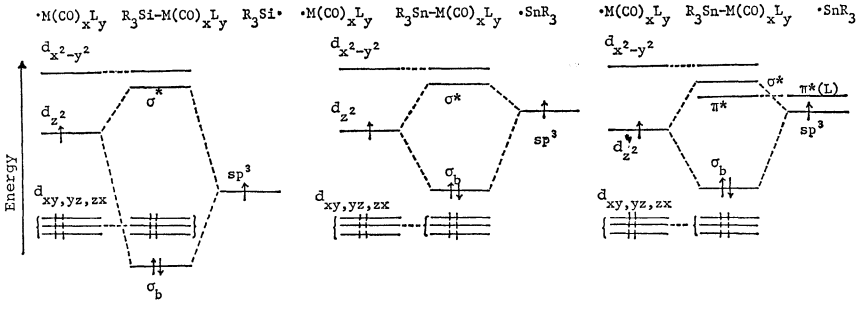

Scheme 1. One-electron energy diagram for R_3M'-$M(CO)_xL_y$.

Table 1. Electronic absorption spectral data

Complex	λ_{max}/nm (ε/M^{-1} cm^{-1})	
Me_3Sn-$Mn(CO)_5$(I)	230 (19000) [a]	
$Me_2Sn[Mn(CO)_5]_2$(II)	230 (22200), [a]	320 (17000)
$MeSn[Mn(CO)_5]_3$(III)	230 (38000), [a]	385 (14700)
Me_3Sn-$Mn(CO)_3L_2$(IV)	230 (21900), [a]	270 sh
Me_3Sn-$Mn(CO)_4L$(V)	230 (19600), [a]	270 sh
$Me_2Sn[Mn(CO)_4L]_2$(VI)	230 (18400), [a] 320 (14200)	265 sh
$P(OPh)_3$	265 (1550)	

a) Shoulder in hexane solution.

scopic studies have shown that the Sn–Mn bond strength is influenced by replacing the carbonyl in R_3Sn–$Mn(CO)_5$ with triphenylphosphine and its congeners.[4l,4m] The present study was undertaken to demonstrate how the photochemistry of a series of Me_3Sn–$Mn(CO)_{5-x}[P(OPh)_3]_x$ or $Me_{3-x}Sn[Mn(CO)_5]_{x+1}$ (x= 0, 1, and 2) is dependent on change in substituents and to clarify the fate of photochemically generated unstable manganese carbonyl intermediates. A preliminary account appeared elsewhere.[4p]

Experimental

All the syntheses were made under a purified nitrogen atmosphere. Photolyses were performed under a purified argon atmosphere with stirring in a Pyrex reaction vessel in which a Riko 100 W water-cooled high pressure Hg lamp was inserted. No filter was used to isolate particular emission from the Hg lamp. IR spectra were recorded on a JASCO-701G infrared spectrometer with 0.1 mm NaCl windowed liquid cells. Absorption spectra were obtained with a Shimadzu MPS-5000 spectrometer with 1 mm quartz cells. CH_2Cl_2 was employed as a solvent. Absorption data are collated in Table 1.

Materials. Me_3Sn–$Mn(CO)_5$ (I), $Me_2Sn[Mn(CO)_5]_2$ (II), $MeSn[Mn(CO)_5]_3$ (III), and Me_3Sn–$Mn(CO)_3[P(OPh)_3]_2$ (IV) (hereafter L denotes triphenyl phosphite) were prepared as described elsewhere.[4] Me_3Sn–$Mn(CO)_4L$ (V) and $Me_2Sn[Mn(CO)_4L]_2$ (VI) were obtained as follows: 1.4 g (1.5 mmol) of $[Mn(CO)_4L]_2$[7] was dissolved in 30 cm^3 of THF and was reduced to $NaMn(CO)_4L$ by stirring over 1% sodium amalgam. The pale yellow supernatant solution was decanted into a flask and to this was added 0.6 g (3 mmol) of Me_3SnCl or 0.35 g (1.5 mmol) of Me_2SnCl_2 in 25 cm^3 of THF with stirring. The mixture was stirred overnight. The resulting pale yellow solution was filtered by using a fine porosity glass frit and the solvent was vacuum-stripped to leave a pale brown oil. For V, the oil was extracted with hexane and the hexane was almost distilled off at reduced pressure to afford 1.5 g of pale yellow crystals (yield: 78%). For VI, the oil was extracted with hot hexane and the solvent was partially vacuum-stripped to give 1.0 g of pale yellow crystals (Yield: 60%). ν(CO)/cm^{-1} in benzene for V: 2048(w) and 1957(vs); for VI: 2088(vw), 2059(vw), 2036(w), 1990(m,sh), 1970(vs), and 1955(s, sh).

Photolysis of I and V. Each 1.0 g sample was dissolved in 50 cm^3 of dried benzene and was irradiated for more than 15 h, but no appreciable change other than decomposition was detected by IR. More than 95% of I was left intact and about 20% of V was decomposed after 15 h irradiation (based on IR spectra).

Photolysis of II. A 1.0 g sample of II was dissolved in 50 cm^3 of benzene and was photolyzed for 8 h. An IR monitoring showed that II was partially converted into other manganese carbonyl complexes. The solvent was removed under a reduced pressure and the residue was purified by column chromatography over Florisil. An yellow band was eluted with petroleum ether and recrystallization from the same solvent gave a small amount of $Mn_2(CO)_{10}$ (yield: more than 50 mg).

Photolysis of III. A 0.2 g sample of III was dissolved in 40 cm^3 of benzene and the solution was photolyzed for 20 min. An IR monitoring indicated complete digestion of III. Similar work up as in the case of II gave 30 mg of $Mn_2(CO)_{10}$.

Photolysis of IV. A 1.0 g sample of IV was dissolved in 50 cm^3 of benzene and photolysed for 8 h. After the solution was filtered, the solvent was distilled off at reduced pressure to leave a pale brown oil. The oil was dissolved in a minimum amount of benzene and was chromatographed over Florisil (60—100 mesh). Hexane was used as the first eluent. From the first fraction a small amount of V (40 mg) was obtained. Then, a hexane–benzene (1:2) mixture eluted the second, third, and fourth fractions. About 300 mg of the starting material IV was recovered from the second fraction. After the solvents were distilled off from the third and fourth fractions, the pale yellow oil was dissolved in a small amount of benzene and to this was added cyclohexane without agitation. The mixture was stored in a refrigerator for several weeks to yield 30 mg of $(PhO)_2P(OC_6H_4)Mn(CO)_2L_2$ (**1**),[4p] 70 mg of *fac-cis*-$(PhO)_2P(OC_6H_4)Mn(CO)_3L$ (**2**),[8] and 50 mg of IV. Finally an yellow band was eluted with $CHCl_3$ and recrystallization from benzene gave 15 mg of yellow crystals (**3**). Elemental analyses of **1**. Found: C, 64.24; H, 3.90; P, 8.73%. Calcd for $C_{56}H_{44}MnO_{11}P_3$: C, 64.62; H, 4.26; P, 8.93%.

Photolysis of VI. A 0.6 g sample of VI was dissolved in 50 cm^3 of benzene and the solution was irradiated for 6 h. After similar work up as in the case of IV, the products were separated by column chromatography over Florisil. The first fraction was eluted with hexane to afford a small amount of oil (about 10 mg). The IR spectrum of this oil was consistent with that of authentic $(PhO)_2P(OC_6H_4)Mn(CO)_4$ (**4**).[9] An yellow band was then eluted with ethanol. Recrystallization from benzene–petroleum ether gave 15 mg of yellow crystals (**3**).[10]

Yields for photolysis products were averaged for several runs for IV and VI and IR data for photolysis products are given in Table 2.

Photolysis of Orthometalated Products. As a typical example, the photolysis of **2** is described. A 0.27 g sample of **2** was dissolved in 40 cm^3 of benzene and was photolyzed for 3 h. The solvent was removed under a reduced pressure to leave a pale brown oil. The oil was dissolved in a minimum amount of benzene and the solution was loaded on a Florisil column. From the first fraction eluted with petroleum ether, 12 mg of **4** was obtained. The second and third fractions were eluted with hexane–benzene (1:1) and were carefully recrystallized as in the photolysis of IV from benzene–petroleum ether to give 16 mg of **1**, 16 mg of **2** and 38 mg of *mer-trans*-$(PhO)_2P(OC_6H_4)Mn(CO)_3L$ (**5**).[11] The fourth fraction was eluted with chloroform and recrystallization from benzene gave a small amount of yellow crystals (**3**).

Photolysis of IV in CCl_4. A 1.0 g sample of IV was dissolved in 50 cm^3 of CCl_4 and the solution was photolyzed for 2 h. After the solvent was vacuum-stripped, the resulting yellow solid was subjected to column chromatography

Table 2. IR data for photolysis products in a Nujol mull

Products	ν(CO)/cm^{-1}	Characteristic peaks of orthometalated $P(OPh)_3$[a] (ν/cm^{-1})
$(PhO)_2\overline{P(OC_6H_4)}\overline{Mn(CO)_2L_2}$ (**1**)	1980(vs), 1920(vs)	1103(m), 951(m), 800(m)
$(PhO)_2\overline{P(OC_6H_4)}\overline{Mn(CO)_3L}$ (**2**)	2031(vs), 1967(vs), 1943(vs)	1101(m), 952(s), 805(m)
Yellow crystal (**3**)	2068(w), 1987(vs), 1940(vs)	
$(PhO)_2\overline{P(OC_6H_4)}\overline{Mn(CO)_4}$ (**4**)	2085(m), 2002(s), 1975(vs), 1962(s)	1101(m), 960(m,sh), 798(m)

a) G. W. Parshall, W. H. Knoth, and R. A. Schunn, *J. Am. Chem. Soc.*, **91**, 4990 (1969); J. L. Levison and S. D. Robinson, *J. Chem. Soc., A*, **1970**, 639; M. Y. Darensbourg, D. J. Darensbourg, and D. Drew, *J. Organomet. Chem.*, **73**, C25 (1974).

Table 3. Atomic positional parameters for **1**[a]

Atom	x	y	z	B_{eq}/Å^2	Atom	x	y	z	B_{eq}/Å^2
Mn	−223(1)	2480(1)	503(1)	3.7	C212	3627(8)	908(3)	2629(9)	5.2
P1	−1111(2)	2503(1)	2115(2)	3.9	C213	4454(9)	422(3)	3104(10)	6.6
P2	343(2)	1635(1)	890(2)	3.9	C214	4171(10)	0(3)	2208(12)	8.0
P3	−260(2)	3331(1)	532(2)	3.7	C215	3080(10)	54(3)	813(11)	7.8
C1	673(8)	2431(3)	−661(8)	4.6	C216	2229(9)	542(3)	301(9)	6.0
C2	−1907(8)	2514(3)	−1007(8)	4.6	C221	−1434(8)	1303(3)	−1648(7)	3.9
O1	1171(6)	2378(2)	−1458(6)	6.3	C222	−2834(8)	1256(3)	−2142(9)	5.2
O2	−2998(6)	2560(2)	−1967(6)	6.8	C223	−3631(9)	1316(3)	−3697(9)	6.0
O11	90(5)	2513(2)	3737(5)	4.7	C224	−3036(9)	1420(3)	−4641(9)	6.1
O12	−2210(5)	3003(2)	1983(5)	4.4	C225	−1646(9)	1464(3)	−4077(8)	5.4
O13	−1801(5)	2031(2)	2457(5)	5.0	C226	−773(9)	1401(3)	−2531(8)	4.7
O21	1748(5)	1440(2)	749(5)	4.8	C231	932(8)	957(3)	3304(8)	4.3
O22	−668(5)	1225(2)	−101(5)	4.2	C232	635(8)	480(3)	2656(9)	5.5
O23	591(6)	1423(2)	2464(5)	5.4	C233	1048(10)	32(3)	3595(10)	6.8
O31	949(5)	3612(2)	454(5)	4.5	C234	1698(11)	73(4)	5120(11)	7.8
O32	−1641(5)	3623(2)	−803(5)	4.6	C235	1946(11)	563(4)	5744(10)	7.8
O33	−244(5)	3615(2)	1963(5)	4.6	C236	1564(9)	1020(3)	4799(8)	6.0
C111	1414(8)	2498(3)	3773(8)	4.6	C311	1534(8)	3562(3)	−551(9)	4.3
C112	1558(7)	2481(3)	2445(7)	4.0	C312	2963(9)	3482(3)	119(9)	5.4
C113	2920(8)	2459(3)	2588(9)	5.3	C313	3676(10)	3450(3)	−756(11)	7.4
C114	4056(8)	2455(3)	4016(11)	7.2	C314	2925(11)	3512(4)	−2304(12)	8.1
C115	3806(9)	2471(3)	5299(10)	7.0	C315	1481(11)	3599(3)	−2954(9)	7.1
C116	2479(9)	2486(3)	5199(9)	6.0	C316	732(10)	3631(3)	−2067(8)	5.8
C121	−2541(8)	3222(3)	3095(8)	4.6	C321	−2259(8)	4145(3)	−912(8)	4.2
C122	−2360(11)	2945(4)	4360(10)	8.0	C322	−3589(9)	4194(3)	−1084(10)	6.5
C123	−2783(12)	3237(5)	5361(10)	9.5	C323	−4277(10)	4705(4)	−1238(12)	8.7
C124	−3287(11)	3759(4)	5090(11)	9.3	C324	−3590(11)	5138(3)	−1193(11)	8.0
C125	−3435(13)	4010(4)	3822(11)	10.1	C325	−2258(10)	5059(3)	−1027(10)	7.4
C126	−3052(11)	3733(3)	2811(11)	7.9	C326	−1548(9)	4545(3)	−925(10)	5.8
C131	−3016(8)	1842(3)	1493(8)	4.8	C331	582(9)	3992(3)	2814(8)	4.9
C132	−4116(8)	2174(3)	438(9)	6.4	C332	−148(12)	4463(3)	2821(11)	8.0
C133	−5319(10)	1956(4)	−462(11)	7.9	C333	630(14)	4842(4)	3722(12)	10.3
C134	−5402(10)	1432(4)	−296(11)	8.1	C334	2041(14)	4705(4)	4481(11)	10.4
C135	−4264(10)	1104(4)	788(10)	7.2	C335	2793(12)	4215(4)	4495(10)	9.2
C136	−3024(10)	1312(3)	1710(9)	5.9	C336	1986(9)	3833(3)	3593(8)	5.8
C211	2557(8)	942(3)	1248(9)	4.7					

a) Positional parameters are multiplied by 10^4 and thermal parameters are given by the equivalent temperature factors.

(Florisil). The first fraction was eluted with hexane–benzene (1:1). Recrystallization from hexane–chloroform gave 220 mg of *mer-trans*-$ClMn(CO)_3L_2$.[12] The second fraction was also eluted with hexane–benzene (1:1) and recrystallization from hexane–chloroform yielded 10 mg of *fac-cis*-$ClMn(CO)_3L_2$.[12]

Photolysis of VI in CCl_4. A 0.5 g sample of VI was dissolved in 30 cm^3 of CCl_4 and the solution was photolyzed for 2 h. Similar work up as above gave 10 mg of *cis*-$ClMn(CO)_4L$ and 100 mg of *mer-trans*-$ClMn(CO)_3L_2$.[12]

Table 4. Atomic positional parameters for 2[a)]

Atom	x	y	z	B_{eq}/Å^2	Atom	x	y	z	B_{eq}/Å^2
Mn	2769(1)	585(1)	1243(1)	2.5	C126	1871(2)	2293(2)	3426(6)	3.3
P1	2233(1)	1104(1)	2279(2)	2.4	C131	2456(2)	1026(2)	4678(6)	2.9
P2	2543(1)	−95(1)	2400(2)	2.4	C132	2914(3)	1311(3)	4641(6)	3.6
C1	3107(2)	163(2)	179(6)	3.3	C133	3263(3)	1247(3)	5647(7)	4.4
O1	3322(2)	−106(2)	−525(5)	5.0	C134	3157(3)	917(3)	6634(7)	4.7
C2	3356(2)	744(2)	2094(6)	3.1	C135	2685(3)	642(3)	6641(6)	4.3
O2	3737(2)	848(2)	2591(5)	4.3	C136	2325(3)	692(2)	5655(6)	3.5
C3	2868(3)	1109(2)	145(6)	3.3	C211	1653(2)	−329(2)	3769(6)	2.8
O3	2927(2)	1437(2)	−571(4)	4.7	C212	1135(3)	−319(3)	3389(7)	3.7
O11	1653(1)	1025(2)	1769(4)	2.9	C213	771(3)	−585(3)	4148(8)	4.8
O12	2336(1)	1711(1)	2057(4)	2.9	C214	935(3)	−843(3)	5226(8)	5.1
O13	2087(1)	1072(2)	3726(4)	3.0	C215	1461(3)	−835(3)	5572(7)	4.7
O21	1985(1)	−30(1)	2994(4)	2.9	C216	1832(3)	−575(2)	4841(6)	3.6
O22	2531(2)	−617(1)	1590(4)	2.9	C221	2303(2)	−1087(2)	2020(5)	2.5
O23	2862(1)	−266(2)	3633(4)	2.9	C222	1799(2)	−1182(2)	1681(6)	3.0
C111	1615(2)	679(2)	753(6)	2.7	C223	1564(2)	−1653(2)	2067(6)	3.2
C112	2061(2)	423(2)	358(6)	2.7	C224	1856(2)	−2010(2)	2774(6)	3.2
C113	1988(3)	77(2)	−668(6)	3.6	C225	2372(2)	−1899(2)	3092(6)	3.1
C114	1492(3)	15(3)	−1211(7)	4.1	C226	2607(2)	−1432(2)	2718(6)	2.7
C115	1058(3)	282(3)	−767(7)	4.3	C231	3399(2)	−342(2)	3718(7)	3.4
C116	1118(3)	624(2)	268(6)	3.5	C232	3600(3)	−293(3)	4928(8)	5.3
C121	1940(2)	2088(2)	2246(6)	2.7	C233	4149(3)	−372(3)	5070(9)	6.9
C122	1662(2)	2240(2)	1200(6)	3.4	C234	4445(3)	−486(3)	4042(10)	7.1
C123	1265(3)	2618(3)	1372(7)	4.2	C235	4234(3)	−543(3)	2861(9)	5.9
C124	1185(2)	2834(2)	2546(7)	3.9	C236	3694(3)	−473(3)	2689(8)	4.4
C125	1480(3)	2681(3)	3569(7)	4.0					

a) Positional parameters are multiplied by 10^4 and thermal parameters are given by the equivalent temperature factors.

X-Ray Molecular Structure Analysis of **1**. Colorless crystals were grown up from hexane–benzene. A crystal of approximate dimensions $0.26\times0.19\times0.07$ mm^3 was mounted on a Rigaku AFC-5 automated four circle diffractometer equipped with graphite monochromated Mo $K\alpha$ radiation (λ=0.71073 Å). The crystal belongs to the triclinic system with unit cell dimensions a=10.820(3), b=25.943(3), c=10.061(2) Å, α=90.61(1), β=115.26(1), γ=82.77(1)°, V=2530.8(10) Å^3, and Z=2. A total of 4199 independent reflections with $|F_o|>3\sigma(|F_o|)$ were obtained at room temperature using the θ-2θ scan technique up to 2θ=50°. No absorption correction was applied. The structure was solved by the standard heavy atom method and refined based on $P\bar{1}$ space group by the use of a UNICS-III program package[13] and computers (HITAC M-180 and M-200H) at Institute for Molecular Science. A series of least-squares refinements for 71 nonhydrogen atoms with anisotropic temperature factors reduced R and R_w to 0.069, where anomalous dispersion correction for Mn and P was applied. The final positional parameters are listed in Table 3. The lists of thermal parameters and F_o and F_c are deposited as Document No. 8304 at the Chemical Society of Japan.

X-Ray Molecular Structure Analysis of **2**. Colorless crystals were obtained from cyclohexane–petroleum ether. Weissenberg photographs using Cu K_α indicated 4/m Laue symmetry. A crystal of approximate dimensions $0.24\times0.24\times0.24$ mm^3 was mounted on a Rigaku AFC-5 automated four circle diffractometer. A preliminary reflection data collection revealed systematic absences $h00$, $0k0$, and $00l$ for h or k or l=2n+1 and $hk0$ for $h+k$=2n+1, which define the tetragonal space group $P4_2/n$ (C_{4h}^4; No 86). The lattice constants, determined by a least-squares fit to 30 high angle (20°≤2θ≤30°) reflections are a=b=25.768(3), c=10.720(3) Å, V=7117.9(24) Å^3, and Z=8. Intensity data were collected at −50 °C by using the same scanning technique as with **1** and a total of 3966 unique reflections with $|F_o|>3\sigma(|F_o|)$ were obtained in the region of h, k, l with $0<h$, k, l up to 2θ=55°. No absorption correction was made. The structure was solved by the standard heavy atom method and refined as mentioned above to give R=0.062 and R_w=0.073 for 51 nonhydrogen atoms with anisotropic temperature factors. Anomalous dispersion correction was applied for Mn and P at the final stage of refinement. Final positional parameters are collected in Table 4 and lists of thermal parameters and F_o and F_c are deposited as Document No. 8304 at the Chemical Society of Japan.

Results and Discussion

Absorption Spectra and Photoreactivity. The absorption spectra for the series of $(CH_3)_{3-x}Sn[Mn(CO)_5]_{x+1}$ (x=0, 1, and 2) are very much dependent on the number of manganese carbonyl groups; a strong absorption is observed at 385 nm besides a very strong absorption at 230 nm for III which possesses three tin-manganese bonds and a strong absorption is detected at 320 nm besides a very strong absorption at 230 nm for II which contains two tin-manganese bonds, while only a very strong absorption is observed at 230 nm for I which possesses only one tin-manganese bond. The very strong absorptions at 230 nm are as-

singable to the Mn to π^*(CO) charge transfer band and those strong absorptions at 385 and 320 nm are assignable to the σ_b(Sn–Mn)→σ^*(Sn–Mn) transition.[1,14] This transition may be hidden behind the very strong charge transfer band at 230 nm for I. Those compounds which possess triphenyl phosphite ligand(s) exhibit an extra absorption around 270 nm. This band is assignable to the π→π^* transition due to the phenyl groups in triphenyl phosphite, since free triphenyl phosphite itself shows this absorption. From a comparison of the absorption spectra for two groups of compounds, that is, I, IV, and V, and II and VI, we are led to the conclusion that the replacement of CO by triphenyl phosphite ligand(s) does not afford any obvious influence on the σ_b→σ^*(Sn–Mn) transition. Thus, the σ_b→σ^*(Sn–Mn) transition energy is in the order Sn–Mn > $Sn\langle^{Mn}_{Mn}$ > $Sn\langle^{Mn}_{Mn}$.

In order to understand the photochemical reactivity of the tin-manganese bonded compounds in connection with the excited states (Scheme 1), it is interesting to examine the relation between the reactivity of Sn–Mn bond and the excitation energy of this bond; the Sn–Mn bonds in III are degraded smoothly under UV irradiation to give $Mn_2(CO)_{10}$. III decomposes rapidly even under a fluorescent room light in CH_2Cl_2. II is partially digested by UV irradiation to yield $Mn_2(CO)_{10}$, while I does not react seemingly. The formation of $Mn_2(CO)_{10}$ from II and III is accounted for in terms of homolytic cleavage of the Sn–Mn bond[5,6,15] and coupling of the resulting ·$Mn(CO)_5$ radicals. Thus, the apparent order of the photoreactivity of Sn–Mn bond is inversely proportional to the order of the σ_b→σ^*(Sn–Mn) transition energy. This order also seems to be related to the light intensity of the lamp used; II and III can be excited by the intense emissions at 313 and 366 nm, respectively, but the emissions effective to excite I is weak in intensity and moreover, the solvent, C_6H_6, absorbs this range of light.

For I, IV, and V, it is unlikely that an electron in the σ_b(Sn–Mn) orbital is excited directly to σ^*(Sn–Mn) by emissions from the present Hg lamp as mentioned above. The observation that IV is more photosensitive than I and V tempts us to speculate an alternative photochemical reaction pathway; IV has an absorption at 270 nm which is assignable to the π→π^*(P(OPh)$_3$) transition and thus, it is conceivable that the low-lying empty π^* orbital should have some connection with the photoreactivity of IV. In this regard, two possible mechanisms come out, that is, an electron in σ_b(Sn–Mn) orbital is excited to the π^*(P(OPh)$_3$) orbital (Scheme 1(c)) or the Sn–Mn bond in IV, which should be enfeebled by the introduction of two bulky triphenyl phosphite ligands in cis positions toward the Sn–Mn bond, is readily labilized by an energy transfer mechanisms from the π→π^*(P(OPh)$_3$) transition.[16] At present, we have no evidence to differentiate these two mechanisms and this point must wait for future experiment.

Reaction Mechanisms of Orthometalation. As was described in the Experimental section, photodegradation of IV and VI in benzene gave orthometalated products (shown in Fig. 1), which contain no tin moiety. Therefore, the process of orthometalation should entail cleavage of the Sn–Mn bond in a certain process of the photochemical reaction. The Sn–Mn bond cleavage in the primary photoprocess was suggested by several experiments: Photolysis of IV in CCl_4 gave $ClMn(CO)_3L_2$ and photolysis of IV together with benzyl chloride in C_6H_6 gave bibenzyl. When the photolysis of IV is conducted in air-saturated benzene, only trace amounts of **1**, **2**, and V were obtained. The yields of **1**, **2**, and V were considerably decreased when argon was bubbled into the benzene solution during the photolysis to purge out gaseous products such as CO and H_2. These lines of evidence indicate that (i) the initial process of photolysis is homolytic cleavage[17] of the Sn–Mn bond to yield Me_3Sn· and ·$Mn(CO)_3L_2$ radicals according to

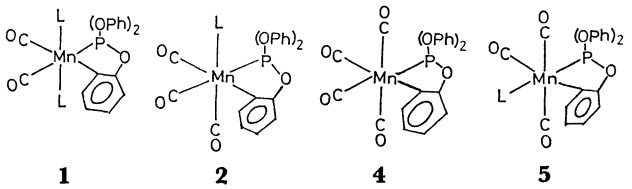

1 **2** **4** **5**

Fig. 1. Schematic pictures of orthometalated manganese carbonyl triphenylphosphite derivatives.

$$Me_3Sn\text{–}Mn(CO)_3L_2 \overset{h\nu}{\rightleftharpoons} Me_3Sn\cdot + \cdot Mn(CO)_3L_2, \quad (1)$$

(ii) the resulting 17-electron manganese carbonyl radical undergoes photochemical or thermal dissociation of the ligand, CO and/or L, according to

$$\cdot Mn(CO)_3L_2 \rightleftharpoons \cdot Mn(CO)_3L + L, \quad (2)$$

$$\cdot Mn(CO)_3L_2 \rightleftharpoons \cdot Mn(CO)_2L_2 + CO, \quad (3)$$

to generate 15-electron intermediates, and (iii) various steps which are likely to account for the formation of orthometalated products **1** and **2** and Me_3Sn–Mn(CO)$_4$L V as are described in Scheme 2 and Scheme 3.

In Scheme 2, the 15-electron intermediates play a key role to abstract hydrogen from a benzene ring in the triphenyl phosphite ligand, while in Scheme 3, the 17-electron radicals which are regenerated from the recombination of the 15-electron intermediates with CO or L abstract hydrogen from a benzene ring in the triphenyl phosphite ligand to form an orthometalated five-membered ring. Although the formations of **4** and Me_3Sn–$Mn(CO)_2L_3$ are expected for both Schemes, we could not isolate these products in spite of our repeated experiments. Me_3Sn–$Mn(CO)_2L_3$ may not be formed, since the steric congestion around the cis positions of the manganese atom toward the Sn–Mn bond, is detrimental to the formation of the Sn–Mn bond or this bond is easily cleaved by UV irradiation. On the other hand, no detection of **4** is enigmatic. Presumably, **4** eluded isolation because of its low yield. In order to differentiate the two schemes, we examined photolyses of orthometalated products, **2** and **5**[11] in benzene. The photolysis of **2** gave **1**, **4**, and **5** and the photolysis of **5** gave **1**, **2**, and **4**. These interconversions should proceed *via* dissociation of the ligand CO or L from the original orthometalated

$$\cdot Mn(CO)_2L_2 \longrightarrow (PhO)_2\overline{P(OC_6H_4)}\overline{Mn(CO)_2L} + 1/2\,H_2, \quad (4)$$

$$\cdot Mn(CO)_3L \longrightarrow (PhO)_2\overline{P(OC_6H_4)}\overline{Mn(CO)_3} + 1/2\,H_2, \quad (5)$$

$$(PhO)_2\overline{P(OC_6H_4)}\overline{Mn(CO)_2L} + L \rightleftharpoons (PhO)_2\overline{P(OC_6H_4)}\overline{Mn(CO)_2L_2}, \quad (6)$$

$$(PhO)_2\overline{P(OC_6H_4)}\overline{Mn(CO)_2L} + CO \rightleftharpoons (PhO)_2\overline{P(OC_6H_4)}\overline{Mn(CO)_3L}, \quad (7)$$

$$(PhO)_2\overline{P(OC_6H_4)}\overline{Mn(CO)_3} + L \rightleftharpoons (PhO)_2\overline{P(OC_6H_4)}\overline{Mn(CO)_3L}, \quad (8)$$

$$(PhO)_2\overline{P(OC_6H_4)}\overline{Mn(CO)_3} + CO \rightleftharpoons (PhO)_2\overline{P(OC_6H_4)}\overline{Mn(CO)_4}, \quad (9)$$

$$\cdot Mn(CO)_2L_2 + \cdot SnMe_3 \rightleftharpoons Me_3Sn\text{-}Mn(CO)_2L_2, \quad (10)$$

$$\cdot Mn(CO)_3L + \cdot SnMe_3 \rightleftharpoons Me_3Sn\text{-}Mn(CO)_3L, \quad (11)$$

$$Me_3Sn\text{-}Mn(CO)_2L_2 + CO \longrightarrow Me_3Sn\text{-}Mn(CO)_3L_2, \quad (12)$$

$$Me_3Sn\text{-}Mn(CO)_3L + CO \longrightarrow Me_3Sn\text{-}Mn(CO)_4L, \quad (13)$$

Scheme 2.

$$\cdot Mn(CO)_2L_2 + L \rightleftharpoons \cdot Mn(CO)_2L_3, \quad (14)$$

$$\cdot Mn(CO)_3L + CO \rightleftharpoons \cdot Mn(CO)_4L, \quad (15)$$

$$\cdot Mn(CO)_3L + L \rightleftharpoons \cdot Mn(CO)_3L_2, \quad (16)$$

$$\cdot Mn(CO)_3L + CO \rightleftharpoons \cdot Mn(CO)_4L, \quad (17)$$

$$\cdot Mn(CO)_2L_3 \longrightarrow (PhO)_2\overline{P(OC_6H_4)}\overline{Mn(CO)_2L_2} + 1/2\,H_2, \quad (18)$$

$$\cdot Mn(CO)_4L \longrightarrow (PhO)_2\overline{P(OC_6H_4)}\overline{Mn(CO)_4} + 1/2\,H_2, \quad (19)$$

$$\cdot Mn(CO)_3L_2 \longrightarrow (PhO)_2\overline{P(OC_6H_4)}\overline{Mn(CO)_3L} + 1/2\,H_2, \quad (20)$$

$$\cdot Mn(CO)_4L + \cdot SnMe_3 \longrightarrow Me_3Sn\text{-}Mn(CO)_4L, \quad (21)$$

$$\cdot Mn(CO)_3L_2 + \cdot SnMe_3 \rightleftharpoons Me_3Sn\text{-}(CO)_3L_2, \quad (22)$$

Scheme 3.

compounds to generate five-coordinate 16-electron intermediates such as those described in Eqs. 4 and 5, and *via* recombination of the intermediates with L or CO to afford six-coordinate products.[18] Thus, it seems reasonable to conclude that five-coordinate orthometalated products can exist with considerable life time. Along the line of this observation together with the reasons described below, we are rather inclined to propose that Scheme 2 represents plausible pathways of the photochemical reaction of $Me_3Sn\text{-}Mn(CO)_3L_2$; first, kinetic studies on the photochemical reactions of $Mn_2(CO)_{10}$ with various phosphines and phosphites demonstrated that disubstituted radicals of the type $\cdot Mn(CO)_3L'_2$ are produced during the photolysis, but there is no precedent, to our knowledge,

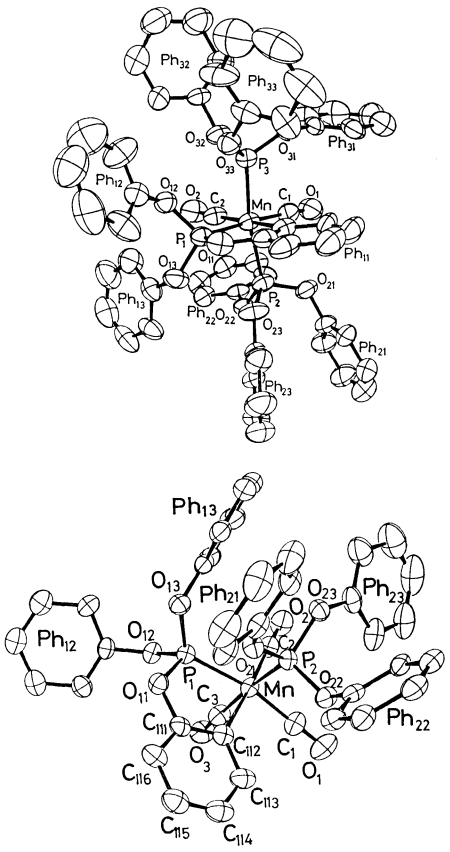

Fig. 2. Molecular structures and atom numbering schemes for **1** (Fig. 2(a)) and for **2** (Fig. 2(b)).

for trisubstituted radicals of the type $\cdot Mn(CO)_2L'_3$, especially for bulky L', the formation of which is mandatory before abstraction of the hydrogen in Scheme 3;[17] second, an ESR study showed that $\cdot Mn(CO)_3L'_2$ radical, which was formed by the photolysis of $Mn_2(CO)_{10}$ with L', possesses a square pyramidal structure where two L' groups occupy basal trans positions. In the present photochemical reaction, it seems certain that the resulting $\cdot Mn(CO)_3L_2$ radical from IV retains its trans geometry as in IV. Therefore, the main product must be **5** even though **5** is partly converted into its isomer **2** if the orthometalated products are formed directly from the 17-electron radical. In spite of this expectation, we could not isolate **5**.

Similar experiments were made for VI as for IV to confirm that the initial photochemical process is homolytic cleavage of the Sn–Mn bond. Photolysis of VI in CCl_4 produced *cis*-$ClMn(CO)_4L$, *mer-trans*-$ClMn(CO)_3L_2$, and a small amount of *fac-cis*-$ClMn(CO)_3L_2$. Photolysis of VI in air-saturated benzene did not afford orthometalated product **4** but gave several unidentified products instead. Photolysis of authentic $ClMn(CO)_4L$ in benzene gave *mer-trans*- and *fac-cis*-$ClMn(CO)_3L_2$. On the basis of these findings, we conclude that the initial photochemical process is homolytic cleavage of one of the Sn–Mn bonds to generate $\cdot Mn(CO)_4L$. Attempts to clarify the fate of the tin moiety have so far been fruitless.

X-Ray Molecular Structure Analyses of ***1*** *and* ***2***. The

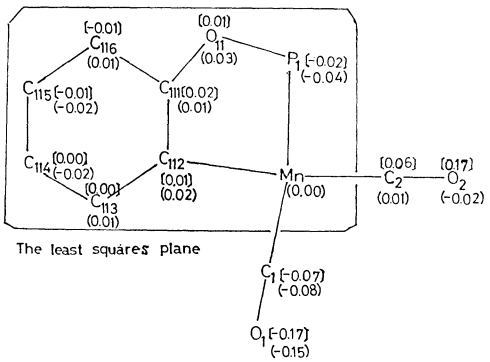

Fig. 3. The least-squares plane and the atom numbering scheme of five-membered orthometalated triphenylphosphite group and the deviations of each atom from the least squares plane; values in [ ] are for **1** and values in ( ) are for **2**.

TABLE 5(a). SELECTED BOND LENGTHS FOR **1**

Bond distance	l/Å	Bond distance	l/Å
$Mn-P_1$	2.208(3)	$O_{11}-C_{111}$	1.414(10)
$Mn-P_2$	2.193(3)	$O_{12}-C_{121}$	1.408(10)
$Mn-P_3$	2.204(3)	$O_{13}-C_{131}$	1.404(10)
$Mn-C_{112}$(Ph)	2.078(8)	$O_{21}-C_{211}$	1.429(10)
$Mn-C_1$	1.805(9)	$O_{22}-C_{221}$	1.419(10)
$Mn-C_2$	1.799(9)	$O_{23}-C_{231}$	1.399(10)
C_1-O_1	1.140(11)	$O_{31}-C_{311}$	1.401(10)
C_2-O_2	1.155(11)	$O_{32}-C_{321}$	1.415(10)
P_1-O_{11}	1.597(6)	$O_{33}-C_{331}$	1.427(10)
P_1-O_{12}	1.611(6)	$C_{111}-C_{112}$	1.410(12)
P_1-O_{13}	1.623(6)	$C_{112}-C_{113}$	1.412(12)
P_2-O_{21}	1.604(6)	$C_{113}-C_{114}$	1.438(14)
P_2-O_{22}	1.631(6)	$C_{114}-C_{115}$	1.426(15)
P_2-O_{23}	1.581(7)	$C_{115}-C_{116}$	1.392(14)
P_3-O_{31}	1.605(6)	$C_{116}-C_{111}$	1.402(13)
P_3-O_{32}	1.623(6)		
P_3-O_{33}	1.604(6)		

TABLE 5(b). SELECTED BOND LENGTHS FOR **2**.

Bond distance	l/Å	Bond distance	l/Å
$Mn-P_1$	2.220(2)	$O_{11}-C_{111}$	1.412(7)
$Mn-P_2$	2.225(2)	$O_{12}-C_{121}$	1.424(8)
$Mn-C_{112}$(Ph)	2.099(6)	$O_{13}-C_{131}$	1.402(7)
$Mn-C_1$	1.801(7)	$O_{21}-C_{211}$	1.419(8)
$Mn-C_2$	1.812(7)	$O_{22}-C_{221}$	1.423(7)
$Mn-C_3$	1.809(7)	$O_{23}-C_{231}$	1.400(8)
C_1-O_1	1.165(8)	$C_{111}-C_{112}$	1.391(9)
C_2-O_2	1.150(8)	$C_{112}-C_{113}$	1.428(9)
C_3-O_3	1.152(8)	$C_{113}-C_{114}$	1.413(10)
P_1-O_{11}	1.605(5)	$C_{114}-C_{115}$	1.396(10)
P_1-O_{12}	1.605(4)	$C_{115}-C_{116}$	1.425(10)
P_1-O_{13}	1.598(4)	$C_{116}-C_{111}$	1.388(9)
P_2-O_{21}	1.582(4)		
P_2-O_{22}	1.601(4)		
P_2-O_{23}	1.618(4)		

molecular structures and atom numbering schemes for **1** and **2** are shown in Fig. 2. The coordination at the manganese atom approximates to a distorted octahedron for both the molecules. The molecular structure of **2** is similar to that of **1** except that the triphenyl phosphite ligand (P_2) has been replaced by a carbonyl group CO(3). The chelating phosphite is coordinated to the manganese atom through both the phosphorus atom and an ortho carbon atom of one of the phenoxyl groups to form a five-membered ring (Fig. 3). The manganese, phosphorus, oxygen, and six carbon atoms in the orthometalated phenyl group are almost coplanar; the greatest deviation of any of these atoms from the least-squares planes is 0.019 Å for **1** and 0.039 Å for **2**. The carbonyl carbon atoms in CO(1)

TABLE 6(a). SELECTED BOND ANGLES FOR **1**

Bond angle	θ/°	Bond angle	θ/°
P_1-Mn-P_2	90.5(1)	$Mn-P_2-O_{21}$	111.9(2)
P_1-Mn-P_3	90.6(1)	$Mn-P_2-O_{22}$	122.4(2)
P_2-Mn-P_3	165.7(1)	$Mn-P_2-O_{23}$	114.7(2)
P_1-Mn-C_{112}	80.0(2)	$Mn-P_3-O_{31}$	122.5(2)
P_2-Mn-C_{112}	82.2(2)	$Mn-P_3-O_{32}$	111.3(2)
P_3-Mn-C_{112}	84.0(2)	$Mn-P_3-O_{33}$	118.0(2)
P_1-Mn-C_1	174.0(3)	$Mn-C_{112}-C_{111}$	117.5(6)
P_1-Mn-C_2	91.3(3)	$Mn-C_{112}-C_{113}$	126.9(6)
P_2-Mn-C_1	86.3(3)	$P_1-O_{11}-C_{111}$	113.5(5)
P_2-Mn-C_2	100.6(3)	$P_1-O_{12}-C_{121}$	128.2(5)
P_3-Mn-C_1	86.3(3)	$P_1-O_{13}-C_{131}$	126.9(5)
P_3-Mn-C_2	93.6(3)	$O_{11}-C_{111}-C_{112}$	119.5(7)
C_1-Mn-C_{112}	94.5(4)	$O_{11}-C_{111}-C_{116}$	113.7(7)
C_2-Mn-C_{112}	171.0(4)	$C_{112}-C_{111}-C_{116}$	126.7(8)
$Mn-C_1-O_1$	175.1(8)	$C_{111}-C_{112}-C_{113}$	115.6(8)
$Mn-C_2-O_2$	176.8(8)	$C_{112}-C_{113}-C_{114}$	120.5(8)
$Mn-P_1-O_{11}$	109.5(2)	$C_{113}-C_{114}-C_{115}$	119.7(9)
$Mn-P_1-O_{12}$	116.4(2)	$C_{114}-C_{115}-C_{116}$	121.3(9)
$Mn-P_1-O_{13}$	124.4(2)	$C_{115}-C_{116}-C_{111}$	116.2(9)

TABLE 6(b). SELECTED BOND ANGLES FOR **2**

Bond angle	θ/°	Bond angle	θ/°
P_1-Mn-P_2	91.9(1)	$Mn-P_2-O_{21}$	112.2(2)
P_1-Mn-C_{112}	78.7(2)	$Mn-P_2-O_{22}$	111.4(2)
P_2-Mn-C_{112}	82.4(2)	$Mn-P_2-O_{23}$	122.5(2)
P_1-Mn-C_1	168.9(2)	$Mn-C_{112}-C_{111}$	119.1(4)
P_1-Mn-C_2	97.6(2)	$Mn-C_{112}-C_{113}$	125.9(5)
P_1-Mn-C_3	87.9(2)	$P_1-O_{11}-C_{111}$	114.1(4)
P_2-Mn-C_1	90.2(2)	$P_1-O_{12}-C_{121}$	121.7(4)
P_2-Mn-C_2	96.7(2)	$P_1-O_{13}-C_{131}$	123.5(4)
P_2-Mn-C_3	170.9(2)	$O_{11}-C_{111}-C_{112}$	118.5(5)
C_1-Mn-C_{112}	90.8(3)	$O_{11}-C_{111}-C_{116}$	114.7(5)
C_2-Mn-C_{112}	176.1(3)	$C_{112}-C_{111}-C_{116}$	126.8(6)
C_3-Mn-C_{112}	88.6(3)	$C_{111}-C_{112}-C_{113}$	114.9(6)
$Mn-C_1-O_1$	179.0(6)	$C_{112}-C_{113}-C_{114}$	120.4(6)
$Mn-C_2-O_2$	177·5(6)	$C_{113}-C_{114}-C_{115}$	121.9(7)
$Mn-C_3-O_3$	178.9(6)	$C_{114}-C_{115}-C_{116}$	118.8(7)
$Mn-P_1-O_{11}$	109.4(2)	$C_{115}-C_{116}-C_{111}$	117.1(6)
$Mn-P_1-O_{12}$	114.2(2)		
$Mn-P_1-O_{13}$	127.0(2)		

and CO(2) are as much as 0.07 Å away for **1** and 0.08 Å away for **2**, respectively, from the least-squares plane (Fig. 3). Although the coplanarity is believed to suggest possible π-electron delocalization over the relevant ring, the bond lengths associated with this ring do not differ significantly from those in the monodentate triphenyl phosphite groups in the same molecule. The selected bond lengths and bond angles are collated in Tables 5 and 6. A comparison of corresponding bond lengths for **1** and **2** indicates that replacement of the triphenyl phosphite on the manganese atom in **1** with a carbonyl leads to significant elongation of the distances from the manganese atom to the phosphorus, carbonyl carbon, and the ortho carbon atoms of the phenyl ring. The Mn–P distances observed for **1** and **2** are considerably shorter than those in analogous triphenylphosphine manganese complexes, 2.279(3)—2.304(4) Å.[19] The Mn–C(phenyl) distances, 2.078(8)—2.099(6) Å, are similar to the generally found Mn–C distances, 2.001—2.097 Å for analogous manganese triphenylphosphine systems.[19] All bond angles relevant to the chelate ring are smaller than normal bond angles of the related atoms, especially the deviation from the ideal angle of 90° is significant in the P_1–Mn–C(phenyl) angles. This angle for **2** is slightly smaller than that of **1**. The two axial triphenyl phosphite groups (we define the plane containing the orthometalated benzene ring as an equatorial plane) are considerably bent toward the orthometalated benzene ring (the angle P_2–Mn–P_3 is 165.7(1)°). The deviation from 180° is supposed to minimize the steric repulsion of the two axial triphenyl phosphite groups with the benzene rings (Ph_{12} and Ph_{13}) in the equatorial triphenyl phosphite group. This deviation is somewhat relaxed in **2** when one of the axial triphenyl phosphite groups is replaced by CO.

Thanks are due to the Institute for Molecular Science for permission to use the AFC-5 automated X-ray diffractometer (the Instrument Center) and the computer (the Computer Center).

References

1) G. L. Geoffroy and M. S. Wrighton, "Organometallic Photochemistry," Academic Press (1979) and references therein.

2) S. Onaka, "Inorganic Photochemistry," ed by the Chemical Society of Japan (1983), Chap. III and references therein.

3) A. J. Cleland, S. A. Fieldhouse, B. H. Freeland, and R. J. O'Brien, *J. Organomet. Chem.*, **32**, C15 (1971); R. C. Job and M. D. Curtis, *Inorg. Chem.*, **12**, 2514 (1973); K. Triplett and M. D. Curtis, *ibid.*, **15**, 431 (1976); H. C. Clark and J. H. Tsai, *ibid.*, **5**, 1407 (1966); T. Foster, K. S. Chen, and J. K. S. Wan, *J. Organomet. Chem.*, **184**, 113 (1980).

4) a) S. Onaka, Y. Sasaki, and H. Sano, *Bull. Chem. Soc. Jpn.*, **44**, 726 (1971); b) S. Onaka, T. Miyamoto, and Y. Sasaki, *ibid.*, **44**, 1851 (1971); c) S. Onaka, *ibid.*, **44**, 2135 (1971); d) S. Onaka, *Chem. Lett.*, **1972**, 101; e) S. Onaka and H. Sano, *Bull. Chem. Soc. Jpn.*, **45**, 1271 (1972); S. Onaka, *Nippon Kagaku Kaishi*, **1972**, 1978; g) Y. Kume, D. Nakamura, M. Kubo, and S. Onaka, *J. Magn. Reson.*, **10**, 58 (1973); h) S. Onaka, *Bull. Chem. Soc. Jpn.*, **46**, 2444 (1973); i) S. Onaka, *Bull. Nagoya Inst. Tech.*, **1973**, 133; j) S. Onaka, *Nippon Kagaku Kaishi*, **1974**, 255; k) S. Onaka, *J. Inorg. Nucl. Chem.*, **36**, 1721 (1974); l) S. Onaka, *Bull. Chem. Soc. Jpn.*, **48**, 319 (1975); m) S. Onaka and H. Sano, *ibid.*, **48**, 258 (1975); n) S. Onaka, Y. Yoshikawa, and H. Yamatera, *J. Organomet. Chem.*, **157**, 187 (1978); o) S. Onaka, *Chem. Lett.*, **1978**, 1163; p) S. Onaka, Y. Kondo, N. Furuichi, and K. Toriumi, *ibid.*, **1980**, 1343; q) S. Onaka, Y. Kondo, K. Toriumi, and T. Ito, *ibid.*, **1980**, 1605.

5) J. C. Luong, R. A. Faltynek, and M. S. Wrighton, *J. Am. Chem. Soc.*, **102**, 7892 (1980).

6) C. L. Reichel and M. S. Wrighton, *Inorg. Chem.*, **19**, 3858 (1980).

7) D. Drew, D. J. Darensbourg, and M. Y. Darensbourg, *Inorg. Chem.*, **14**, 1579 (1975).

8) M. Y. Darensbourg., D. J. Darensbourg, and D. Drew, *J. Organomet. Chem.*, **73**, C25 (1974).

9) R. J. McKinney, R. Hoxmeier, and H. D. Kaesz, *J. Am. Chem. Soc.*, **97**, 3059 (1975).

10) ν(CO) of **3** in $CHCl_3$ is almost identical with that of authentic *mer-trans*-$XMn(CO)_3L_2$ (X=Cl and Br). We suspected at first that a trace amount of the starting material $BrMn(CO)_3L_2$ to synthesize IV is the origin of **3**. However, this possibility is excluded since it was not employed for the synthesis of VI. All the attempts including X-ray molecular structure analysis has so far been fruitless for characterizing this yellow crystal.

11) This product was obtained from the photolysis of $MeMn(CO)_3L_2$. Details of the photochemical reactions of this compound and related compounds will appear in a subsequent paper.

12) R. A. Angelici, F. Basolo, and A. J. Pöe, *J. Am. Chem. Soc.*, **97**, 6042 (1975).

13) T. Sakurai and K. Kobayashi, *Rikagaku Kenkyusho Hokoku (Rept. Inst. Phys. Chem.)*, **55**, 69 (1979).

14) R. A. Levenson and H. B. Gray, *J. Am. Chem. Soc.*, **97**, 6042 (1975).

15) D. L. Morse and M. S. Wrighton, *J. Am. Chem. Soc.*, **98**, 3931 (1976).

16) It is a reasonable question that why V is inert to photoexcitation despite that V shows a spectrum similar to that of IV. To this question, we propose a rationale that the Sn–Mn bond in V is stronger than that of IV[4l,4m] and that the Sn–Mn bond in V is not readily cleaved.

17) M. S. Wrighton and D. Bredensen, *J. Organomet. Chem.*, **50**, C35 (1973); M. S. Wrighton and D. S. Ginley, *J. Am. Chem. Soc.*, **97**, 2065 (1975); D. R. Kidd, C. P. Cheng, and T. L. Brown, *ibid.*, **100**, 4095, 4103 (1978).

18) For an alternative mechanism, one may think of dissociation of the bidentate triphenyl phosphite ligand, which regenerates free triphenyl phosphite ligand, or simple cleavage of the Mn–C(phenyl) bond, which generates "semi-free" triphenyl phosphite and then produces free triphenyl phosphite ligand. However, this mechanism is less likely, because we could not isolate either **1** or **2** or **5** from the prolonged photolysis of **4**. Presumably the five-membered metalation ring is sterically favorable and resists dissociation.[9]

19) R. J. McKinney, C. B. Knobler, B. T. Huie, and H. D. Kaesz, *J. Am. Chem. Soc.*, **99**, 2988 (1977) and references therein.